The Journal of Immunology

RESEARCH ARTICLE | JULY 01 2004

Dendritic Cell Trafficking and Antigen Presentation in the Human Immune Response to *Mycobacterium tuberculosis* [1] FREE

Simeone Marino; ... et. al

J Immunol (2004) 173 (1): 494–506.
https://doi.org/10.4049/jimmunol.173.1.494

Dendritic Cell Trafficking and Antigen Presentation in the Human Immune Response to *Mycobacterium tuberculosis*[1]

Simeone Marino,* Santosh Pawar,† Craig L. Fuller,‡ Todd A. Reinhart,‡ JoAnne L. Flynn,† and Denise E. Kirschner[2]*

***Mycobacterium tuberculosis* (Mtb) is an extraordinarily successful human pathogen, one of the major causes of death by infectious disease worldwide. A key issue for the study of tuberculosis is to understand why individuals infected with Mtb experience different clinical outcomes. To better understand the dynamics of Mtb infection and immunity, we coupled nonhuman primate experiments with a mathematical model we previously developed that qualitatively and quantitatively captures important processes of cellular priming and activation. These processes occur between the lung and the nearest draining lymph node where the key cells mediating this process are the dendritic cells (DC). The nonhuman primate experiments consist of bacteria and cell numbers from tissues of 17 adult cynomolgus macaques (*Macaca fascicularis*) that were infected with Mtb strain Erdman (~25 CFU/animal via bronchoscope). The main result of this work is that delays in either DC migration to the draining lymph node or T cell trafficking to the site of infection can alter the outcome of Mtb infection, defining progression to primary disease or latent infection and reactivated tuberculosis. Our results also support the idea that the development of a new generation of treatment against Mtb should optimally elicit a fast DC turnover at the site of infection, as well as strong activation of DCs for maximal Ag presentation and production of key cytokines. This will induce the most protective T cell response. *The Journal of Immunology*, 2004, 173: 494–506.**

One of the major causes of death by infectious disease worldwide is *Mycobacterium tuberculosis* (Mtb)[3] infection. Despite the fact that one-third of the world population is infected with Mtb, the majority of infected individuals experience an asymptomatic state known as latency, with only 5–10% progressing to active disease or primary tuberculosis (TB). How and why some individuals remain in a latent state while others progress to primary disease or reactivation are still unclear.

Mtb primary infection progression may have a slow time course with reactivation being an even longer process, up to 33 years (1, 2). When active TB develops in humans, infection localization, severity, and outcome are highly variable, and little data exist regarding infection kinetics. A positive purified protein derivative test status indicates infection, and progression from negative to positive purified protein derivative test signifies progression from exposure to infection. Due to the wide time range over which infection can progress to an active state, the time frame for primary disease to manifest ranges from 1 to 5 years (3–6). This represents the time frame within which patients who have been exposed to Mtb likely progress to a state of clinical disease. Individuals exposed to the bacilli who do not progress to active disease are generally believed to contain dormant bacilli; this state is often referred to as latent TB (7).

During infection, macrophages (Mϕs) are the prime target cells for Mtb, which after their activation can both kill intracellular bacteria and participate in a protective Th cell type 1 (Th1) response. As professional APCs, dendritic cells (DCs) play a major role in establishing an effective adaptive response. In fact, there is growing evidence that generation of different types of immune responses is controlled by DCs (8, 9). A novel hypothesis suggests that different DC lineages drive the final commitment of T cells (8, 10–21). However, other evidence suggests that the same subset of DCs can promote either a Th1 or a Th2 response (8). This indicates that DC subsets can induce different Th responses according to a combination of signals. Activation signals can affect the capability of DCs to prime and induce potentially different Th responses. These include the nature (22) and load of microorganism (23), factors released by tissue and inflammatory cells (damage signals) (24–28), physical interactions with other cell types (29), death of infected cells (30), duration of the TCR engagement (8), and pattern recognition receptors (31–33).

DCs and Mtb

Although the role of Mϕs in Mtb infection has been extensively addressed (34), more recent studies (35–40) have focused on the interaction of Mtb with DCs. Elaborating population dynamics of DCs in vivo can help define the role of these cells during Mtb infection. DCs generated from progenitors in the bone marrow migrate into peripheral tissues through the bloodstream. Immature or resting DCs (IDC) are present in high numbers at sites of infection (such as the lung) at the onset of the inflammatory response

*Department of Microbiology and Immunology, University of Michigan Medical School, Ann Arbor, MI 48109; and †Department of Molecular Genetics and Biochemistry, University of Pittsburgh School of Medicine, and ‡Department of Infectious Diseases and Microbiology, University of Pittsburgh Graduate School of Public Health, Pittsburgh, PA 15261

Received for publication February 3, 2004. Accepted for publication April 19, 2004.

The costs of publication of this article were defrayed in part by the payment of page charges. This article must therefore be hereby marked *advertisement* in accordance with 18 U.S.C. Section 1734 solely to indicate this fact.

[1] S.M. and D.E.K. have been supported by grants from National Institutes of Health (NIH)/National Institute of Allergy and Infectious Diseases (NIAID) (HL62119 and HL68526) and from the Biomedical Research Council of University of Michigan Medical School. S.P. and J.L.F. are supported by grants from NIH/NIAID (AI47485) and National Heart, Lung, and Blood Institute (HL62119).

[2] Address correspondence and reprint requests to Dr. Denise E. Kirschner, Department of Microbiology and Immunology, University of Michigan Medical School, 6730 Medical Science Building II, Ann Arbor, MI 48109-0620. E-mail address: kirschne@umich.edu

[3] Abbreviations used in this paper: Mtb, *Mycobacterium tuberculosis*; TB, tuberculosis; Mϕ, macrophage; DC, dendritic cell; IDC, immature DC; MDC, mature DC; DLN, draining lymph node; NHP, nonhuman primate; BAL, bronchoalveolar lavage; Th_P, Th precursor; PRC, partial rank correlation.

0022-1767/04/$02.00

(41–49), and they are specialized for Ag uptake and processing (35, 39, 46–48, 50, 51). After bacterial uptake, DCs change their behavior, as observed both in vitro and in vivo (48), reducing their phagocytic and/or endocytic capability and initiating expression of immune stimulatory molecules (maturation). DC maturation is initiated in nonlymphoid tissues where DCs take up Ag and continues within secondary lymphoid tissues, in particular, the draining lymph node (DLN). Differentiation of IDCs in the DLN leads to a phenotypic change into the mature phenotype (mature DC (MDC)).

Migration (and presumably maturation) of DC from nonlymphoid tissues into DLN is promoted by locally produced inflammatory cytokines and other agents that are generated during local infection or trauma (26, 27, 52). Infection indeed has an effect on homeostatic chemokine expression in the lung (53) and on DC localization into secondary lymphoid tissues by altering expression of chemokines and chemokine receptors (e.g., CCR7 and CCR6) (54). These signals drive DC trafficking and migration first to the lymphatic vessels and then to DLNs via CCL21/6Ckine and other chemokines (e.g., MIP-3β or CCL19, CCL21/6Ckine, CCL20/MIP-3α) released by MDCs in the DLNs (53, 55). IDCs that take up bacteria also express high levels of adhesion molecules (47, 49, 56, 57) that allow migration into DLNs.

Once in the DLN, DCs (MDCs) display a mature phenotype resulting in expression of high levels of long-lived MHC I and MHC II molecules (10, 34, 35, 37, 39) (from 5- to 20-fold over IDCs) that enable more stable presentation of Ag (46). Other molecules that are expressed after maturation are costimulatory molecules including B7 (up to 100-fold) (10, 46), CD40, and Fas (27). Moreover, MDCs produce and enhance expression of CCL18 (pulmonary and activation-regulated chemokine/DC-CK1), a chemokine that specifically attracts naive T cells to DLNs (57–59). The maturation-migration process of DCs is enhanced during Mtb infection, whereas infected Mϕs show little phenotypic change (34, 35, 39, 60).

Before infection, resting Mϕs and IDCs do not produce significant amounts of cytokines (35, 39). Recent studies highlight how, after Mtb infection, MDCs release Th1-inducing cytokine IL-12 in very high amounts (35, 39, 49). On the contrary, infected Mϕs produce mainly anti- and proinflammatory cytokines (e.g., IL-10, TNF-α) (35, 37, 39); thus, during Mtb infection, Mϕs and DCs likely perform different functions. Because MDCs are known to migrate to the DLN for presentation to naive T cells and because they produce IL-12 in a great amount after Mtb uptake, it seems likely that a Th1-type environment is established in the DLN early in the infection process (61, 62). The cytokine environment (e.g., GM-CSF, IL-10, and IL-4) may also play a role in monocyte maturation into either DCs or Mϕs (63), defining cell population phenotypes at the site of infection (64).

To study the dynamics outlined above, we have applied a mathematical model of Mtb infection previously published by our group (65) to determine mechanisms controlling infection outcome. We developed a two-compartment model that qualitatively and quantitatively captures important processes of cellular activation and priming as well as relevant migration patterns between DLN and lung. To guide our work, a nonhuman primate (NHP) model of TB is studied concurrently for data comparison (66, 67). This NHP model has provided data for parameter estimation as well as data for validation of our virtual experiments. Because this study is focused on studying human TB, we must rely on human bronchoalveolar lavage (BAL) fluid and cells as a surrogate marker of immune dynamics in lung. In actuality, the immune response to Mtb occurs in tissue via the development of granulomas. We explore this granuloma response in other work (J. L. Segovia-Juarez, S. Ganguli, and D. E. Kirschner, manuscript in preparation; Ref. 68).[4]

Our main goal here is to address the relevance of trafficking of DCs to and from the DLN in establishing a protective immune response against Mtb. We also compare our virtual human experiments of different infection outcomes in humans during Mtb infection with our NHP experimental data, suggest new experiments, and finally define potential treatment strategies.

Materials and Methods

NHP model

Seventeen adult, simian retrovirus type D-negative cynomolgus macaques (*Macaca fascicularis*) (6–9 years of age; 3.1–9.7 kg) were infected with Mtb strain Erdman, ~25 CFU/animal, via bronchoscope into the right middle or lower lung (67). All animals were individually housed in 4.3-square foot stainless-steel cages equipped with lexan fronts to reduce the potential for aerosol contact between animals. All cages were maintained within a negatively pressurized BioBubble (Colorado Clean Room Company, Fort Collins, CO) located within a biosafety level 3 suite. All animal experimentation guidelines were followed in these studies, and the University of Pittsburgh School of Medicine Institutional Animal Care and Use Committee approved all experimental manipulations and protocols.

BAL was performed monthly (67). Monkeys were euthanized and necropsied either at a predetermined time postinfection or if they developed a rapidly progressing TB. At necropsy, tissue pieces from lung, lymph node, and visible granulomas were placed into sterile RPMI 1640 medium in preweighted tubes, and weight of the tissue was recorded. Tissue was homogenized to obtain single-cell suspensions in a MediMixer (BD Biosciences, San Jose, CA). Ten-fold dilutions of these homogenates, as well as BAL fluid, were plated on 7H10 agar plates (Difco, Detroit, MI), incubated at 37°C and 5% CO_2, and CFU were counted after 4 wk. Cell numbers were determined by trypan blue exclusion in single-cell suspensions from tissues. Flow cytometry was performed on lung, granuloma, and lymph node cell preparations at necropsy to determine the composition of the tissues, as previously described (67, 69). Abs used were anti-CD3 (clone SP34), anti-CD14 (clone MOP9), anti-CD4 (clone SK3), anti-CD11b (clone ICRF44), anti-CD16 (clone 3G8), anti-CD8 (clone SK1), and anti-HLA-DR (clone TU36), all from BD Biosciences (Mountain View, CA).

Staining and quantitation of fascin-positive cells

Immunohistochemical staining of 14-μm tissue sections was performed using anti-fascin (also known as p55) murine mAb (clone 55K-2; DakoCytomation, Carpinteria, CA). Tissue sections from cynomolgus macaques infected with Mtb were pretreated by microwaving for a total of 10 min in 0.01 M sodium citrate (pH 6.0), followed by application of the primary Ab (diluted 1/100 in PBS) for 1 h in a humid chamber at room temperature. Primary Ab was detected with the PicTure-Plus detection system (Zymed Laboratories, San Francisco, CA) using 3,3′-diaminobenzidine as the final substrate. The granuloma size (surface area in square micrometers) and the percentage of fascin-positive cells were quantitated in image capture through an RT Slider Spot camera (Diagnostic Instruments, Sterling Heights, MI) using the MetaView imaging software package (Universal Imaging, Downington, PA). Images of granulomas were acquired through a ×4 objective lens on a Nikon (Melville, NY) E600 research microscope, and the total and nonnecrotic surface areas of the granulomas were measured. Five random images of the cellular portion of each granuloma were captured through a ×60 objective lens, and the total numbers of cells (nuclei) and the numbers of fascin-positive cells were manually counted in each image.

Mathematical model

We study DLN dynamics and compare them with those occurring in the infected lung using an existing mathematical model of the host response to Mtb (65). This model comprises two relevant physiological compartments (the lung and the DLN) and 17 variables: 13 in the lung and 4 in the DLN. The variables in the lung are as follows: Mϕs (resting, activated, and infected), immature or resident DCs, bacteria (both extracellular and intracellular), cytokines (IFN-γ, IL-12, IL-4, and IL-10) and lymphocytes (Th precursor (Th_p), Th1, and Th2). In the DLN compartment, we track MDCs,

[4] S. Ganguli, D. Gammack, and D. E. Kirschner. A metapopulation model of granuloma formation in the lung during infection with *Mycobacterium tuberculosis*. *Submitted for publication.*

lymphocytes (naive T cells (T) and Th_P (Th_P^{LN})), and IL-12. The model formulation and testing is discussed in detail in Ref. 65; however, we briefly outline key interactions included.

Fig. 1 illustrates the model assumptions from Ref. 65. Because we focus on DCs, Ag presentation in the DLN is performed only by MDCs. The migration/maturation process of IDC takes place only after bacterial uptake at the site of infection. We also assume that Mϕs do not play a major role in Ag presentation in the DLN; therefore, only naive T cells and nonpolarized Th cells (Th_P) are present there. Th_P cells (also called Th0 or nonpolarized Th cells) represent a bipotential stage in Th cell differentiation, namely, Th_P (9, 70–72). Although they can be stimulated to produce both Th1-type and Th2-type cytokines, Th1 and Th2 cells are likely already committed. The existence of Th_P is controversial, and indeed this class may encompass a spectrum of cells differentiating from naive to Th1/Th2 phenotypes, as well as memory T cells (9, 62).

Our main hypothesis regarding lymphocyte populations is that the primary cellular output from DLNs is mainly of Th_P type. These cells are then modulated by the local cytokine environment on the way to, and at the site of, infection (26, 27, 64). These cells could also remain in a Th_P state or become memory T cells (however, we do not address memory T cell dynamics in the present model).

Although we do not explicitly account for effector $CD8^+$ T cells (CTLs) in this model, we account for their effects in two key ways. First, we include an extra source of IFN-γ, assumed to come directly from CTLs (73–75), and second, we account for CTL-induced killing of infected Mϕs beyond what is accomplished via Th1 apoptosis. To this end, we assume the action of CTLs is proportional to Th1-effector function (targeting intracellular bacteria); thus, the E:T ratio ($Th1/M_I$) indirectly determines the rate of infected Mϕ killing. T cell killing of infected Mϕs by apoptosis and cytotoxic action is accomplished via the rate k_{14}, and our results indicate that it is crucial in determining infection outcome (65). In other work, we explore the role of CTLs in Mtb infection in a more mechanistic fashion (D. Sud, J. L. Flynn, and D. Kirschner, manuscript in preparation).

For the purpose of this work, we briefly review the virtual latent infection and active TB scenarios and compare them to our NHP experimental data. We also use the mathematical model to perform virtual deletion and depletion experiments and discuss the sets of rates/rate constants that are responsible for leading to different infection outcomes (namely, latency, clearance, active disease, and reactivation). It is the host-pathogen processes governed by these rates/rate constants that are likely targets for further experimental studies. As discussed in Ref. 65, we consider the total bacterial load as the most informative marker of infection progression in our simulations.

Uncertainty and sensitivity analysis of rates/rate constants

Each different cell-cell and cell-cytokine interaction is represented in the model by mechanistic terms with specific rates/rate constants. The effect of a particular term within the system is studied by varying the respective parameter. For example, to study the effect of Ag presentation in the DLN performed by MDC, we vary the parameter accounting for that mechanism in the model over a given biologically relevant range. Setting that parameter to zero (or to very low levels) signifies ineffective or no Ag presentation in the DLN. To systematically study the complex network of interactions, the model parameter space has been fully explored to assess how variations in a single parameter (individual effect) or which combination of parameters (multiple effect) might discriminate between different infection outcomes.

To quantify the importance of each mechanism, all effects are evaluated using statistical techniques called uncertainty and sensitivity analyses. They are implemented in C code and based on Latin hypercube sampling and partial rank correlation (PRC), respectively (76–79). The Latin hypercube sampling method explores effects of uncertainties in our parameter estimation on model outcomes and allows for simultaneous random, evenly distributed sampling of each parameter within a defined range. The correlation between parameter variation and a specific variable outcome (for example, how Ag presentation in the DLN correlates with total bacterial load) is then computed by combining the uncertainty analyses with PRC. PRC coefficients tell us the nature and degree of sensitivity between different mechanisms within the model, and help us to identify and quantify the mechanisms that are critical to affecting the outcome when varied.

Virtual deletion and depletion experiments

One of the main advantages of a mathematical model is the ability to manipulate the equations to ask questions about interactions and rates within the system. For example, we can easily perform both virtual deletion and depletion experiments and compare the results with known experimental data in mice as well as perform new experiments that may be difficult or presently impossible to perform (for example, DC and Th1 virtual deletion and depletion experiments).

Virtual deletion experiments mimic knockout (disruption) experiments, removing an element from the system from the beginning of the simulation, before the bacteria enter the host. This analysis guides our understanding as to which elements may be relevant in controlling initial infection and establishing latency. We can also simulate depletion experiments, for example, after the system has achieved latency, by setting to zero the parameter related to cytokine production (mimic Ab-neutralizing effects). This allows us to determine what elements control maintenance of the latent state.

Results

Measure units: scaling lung and lymph node compartments

Our system is developed to model human TB, both at the site of infection and in the DLN. Most human experimental data in the lung come from BAL cellular and fluid samples (80–82). BAL

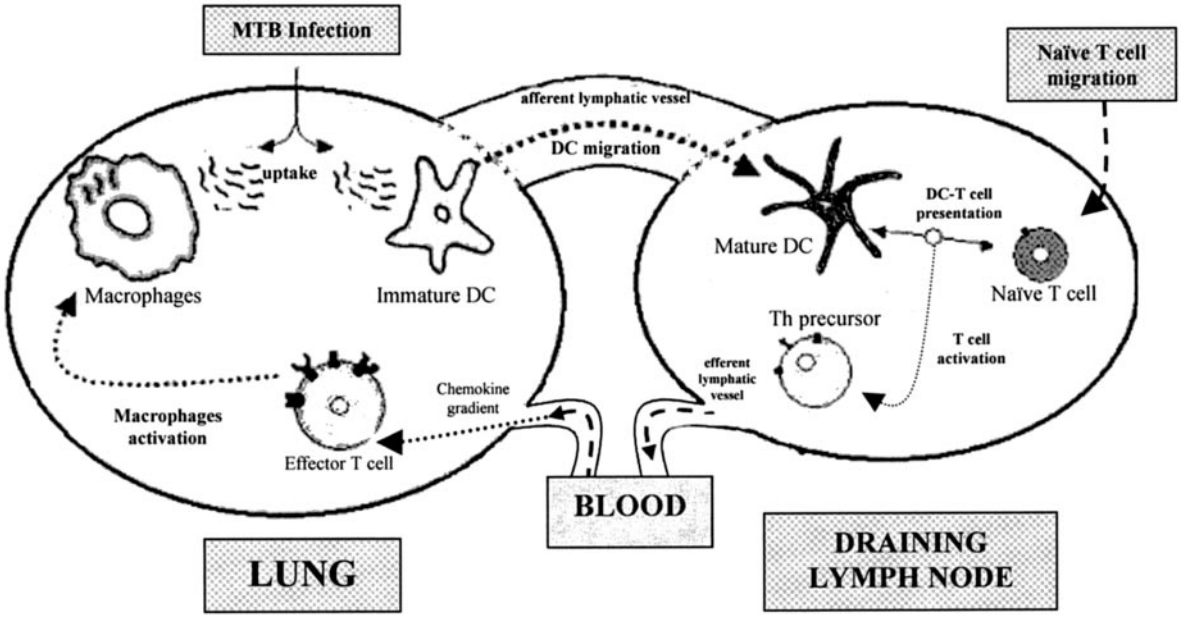

FIGURE 1. Cartoon representing the mathematical model of Mtb-immune dynamics from Ref. 65. Two compartments of lung and lymph node are represented with relevant cell types in each. DC uptake, trafficking, and presentation are represented, as well as related processes. For further details, see Ref. 65.

Table I. *Average cell recovery from tissue of* M. tuberculosis*-infected NHPs at necropsy*[a]

Location	Cell No.
Total lung lobes[b]	2×10^6–2×10^7/cm^3
Hilar lymph node	3×10^7 (total)
1 lung granuloma (visible)	1–4×10^6
BAL[c]	2×10^6–2×10^7 (total)

[a] Data were averaged from six necropsies of monkeys at various stages of disease (M72-00, M112-01, M152-00, M146-00, M153-00, M150-00. See Ref. 67 for details.
[b] Lower end in monkeys with minimal disease.
[c] Higher end in monkeys with rapid disease.

measurements as a surrogate of events in the lungs have some drawbacks. For example, they overestimate Mϕ population size and activity (i.e., cytokine production) in the lower respiratory tract, underestimating DC and lymphocyte populations. Certainly BAL samples are not informative regarding the DLN.

To scale lung and lymph node compartment cell trafficking, we use volumetric measure units. Table I illustrates data on the average cell recovery from tissue of Mtb-infected NHPs at necropsy. A reasonable upper bound of hilar lymph node volume might be the volume of perihepatic lymph node, within the order of 3.4 ± 2.4 ml (83), where 1 ml = 1 cm^3. Based on visual experience of our NHP necropsies, a more reasonable upper limit for hilar lymph node is probably 1 cm^3 (sometimes even smaller). Total cells recovered from the hilar lymph node of Mtb-infected NHPs at necropsy is on the order of 10^7 (Table I), approximately on the order of the number of cells recovered in a cubic centimeter of the lung lobes (and also on the order of total BAL recovery). Variability in cell numbers recovered from lung tissue is due in part to differences in disease status, NHP anatomy, and perfusion at necropsy.

We can reasonably use cells per cubic centimeter as our cell population measure unit (both in the lung and in the lymph node). We assume there exists an average initial cell population of 10^4 in the hilar lymph node and 10^6 cells in 1 cm^3 of the lung (initially, there are fewer cells in the lung when there is no infection, and thus no inflammation is present). We also calibrate initial conditions of our virtual infection model to match a hypothetical cell distribution in the two compartments of lung and DLN (see Ref. 65). The initial bacterial inoculum is 25 bacteria (derived from the NHP experiment protocol). Each equation of the model thus represents the incremental variation of a certain quantity over time (day): picograms per milliliter ($\times 10^6$ cells) for cytokine concentrations, and cells per cubic centimeter of tissue for cellular variables.

Review of the latency scenario

Because our goal is to use the mathematical model to determine which factors are crucial in establishing and maintaining latency, we briefly review the latency scenario obtained with our model simulations (further details about this and other virtual experiments, such as primary TB, can be found in Ref. 65). We defined two bacterial subpopulations: intracellular and extracellular bacteria. Intracellular bacteria are those that have been internalized by resting Mϕs and IDCs, whereas all other bacteria are considered extracellular. These simulations were basically generated with the rate/rate constants used in Ref. 65. We change only a few parameters to obtain more realistic bacterial population numbers.

Initial stages of latency are similar to primary TB up to day 250 (see Ref. 65). A sustained Mϕ activation (see Fig. 2) coupled with a more efficient cell-mediated response result in lower levels of intracellular bacteria (at $\sim 4 \times 10^3$ cells/cm^3; see Fig. 3). The number of infected Mϕs is small, and total bacterial load is represented by intracellular bacteria housed within infected Mϕs (extracellular bacterial load is almost zero; see Fig. 3). The few extracellular bacteria are readily internalized by both Mϕs and IDCs and are also taken up by activated Mϕs, thus containing infection. Bacteria are completely controlled, and latency is achieved by $\sim$200 days. Overall, there is a 60% increase in healthy resting Mϕs in the lung.

Cytokine levels (Fig. 3) are predominantly of type 1 and are sustained after latency has been achieved. Our model simulations reflect the order of magnitude found in BAL samples and qualitatively represent the cytokine environment at the site of infection (84–86). IL-10 adequately counterregulates IFN-γ and IL-12 activity, down-regulating Mϕ activation. These cytokines reach a stable level, with IFN-γ 2-fold higher (1.4×10^2 pg/ml) than IL-12. As expected, IL-4 levels are much lower than those of IFN-γ and IL-12 (87).

A protective Th1 cellular response is mounted after 200 days, with Th1 cells peaking at around 4×10^3 cells/cm^3 after 1 year, and then decreasing to very low levels once latency has been established (Fig. 4). Although very low, these levels are crucial to maintaining latency (as is confirmed by virtual depletion experiments; see *Virtual depletion experiments*). After 200 days, Th_p

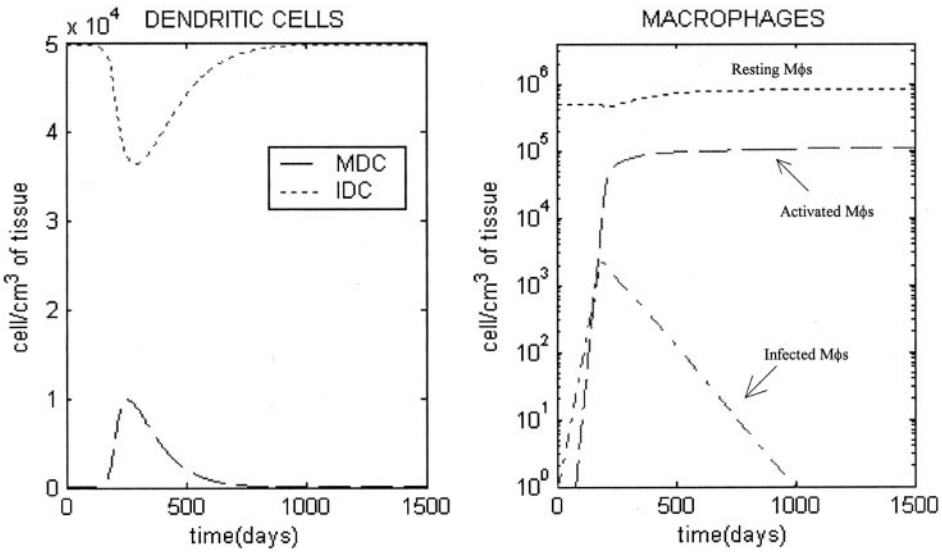

FIGURE 2. DC (IDC and MDC) and Mϕ population (log scale) during initial infection developing into latent infection (1000 days).

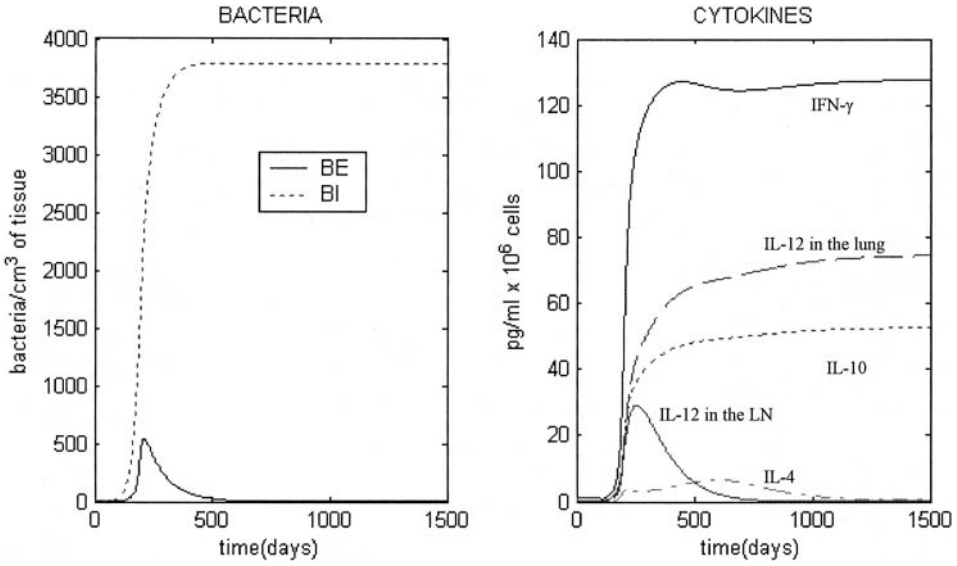

FIGURE 3. Bacterial dynamics (extracellular and intracellular; 1500 days) and cytokines (IFN-γ, IL-12, IL-10, IL-4, and IL-12 in the DLN; 1500 days) during latency. The number of intracellular and extracellular bacteria in 1 cm^3 of the lung tissue refer to a granulomatous region.

cells in the DLN (Fig. 4) decrease (10- to 15-fold lower than primary TB, see Ref. 65), whereas Th_P in the lung continue increasing and remain higher than those in the DLN, stabilizing much later than other cells in the system. This suggests that, during peak infection, a faster migration of Th_P cells from the DLNs to the lung may be one explanation for the host to contain bacteria during latency. DC levels return to baseline after latency is achieved (Fig. 2), suggesting how their role is necessary for both establishing (via MDC presentation in the DLN) and maintaining latency (with IDCs as sentinels for further extracellular bacteria invasion). Virtual deletion and depletion experiments confirm these findings (see below).

NHP data vs mathematical model simulations

We compared data collected from NHP experiments with our model results. To perform a correct comparison, we made some assumptions. Our measure unit is number of cells per gram (or cubic centimeter) of tissue in the lung or lymph node. The number of cells is likely to be different in a granuloma vs nearby nongranulomatous tissue, and this complicates our ability to compare directly, depending on from where the sample is taken. Our NHP data represent both granulomatous and nearby nongranulomatous tissue (monocyte and lymphocyte gates and CFU numbers).

Table II shows data gated from monocyte gate ($CD11b^+$) of Mtb-infected lung of six representative NHPs. These NHPs were sacrificed at different days postinfection (from 60 to 450 days), and each experienced a different infection outcome: from minimal infection with no symptoms (latency or chronic TB) to active TB (from moderate to advanced infection) (see Table I in Ref. 67 for details about monkey labels and stage of disease at necropsy for each monkey). Disease status determined the time of necropsy. BAL measures give larger intervals for cell numbers than lung lobe samples, confirming that BAL is more variable and in general not a robust measure.

The cell types in 1 g of lung tissue represented in our model are Mϕs, IDCs, and lymphocytes. They account for ~20–40% of the total cell population in the lung (type 1 and type 2 pneumocytes, as well as endothelial cells represent a very high percentage). The cell types in 1 g of lymph node tissue represented in our mathematical model are MDCs and lymphocytes. They represent approximately between 10 and 20% of the total cell population in the lymph node (B cells, follicular DCs, and endothelial cells represent

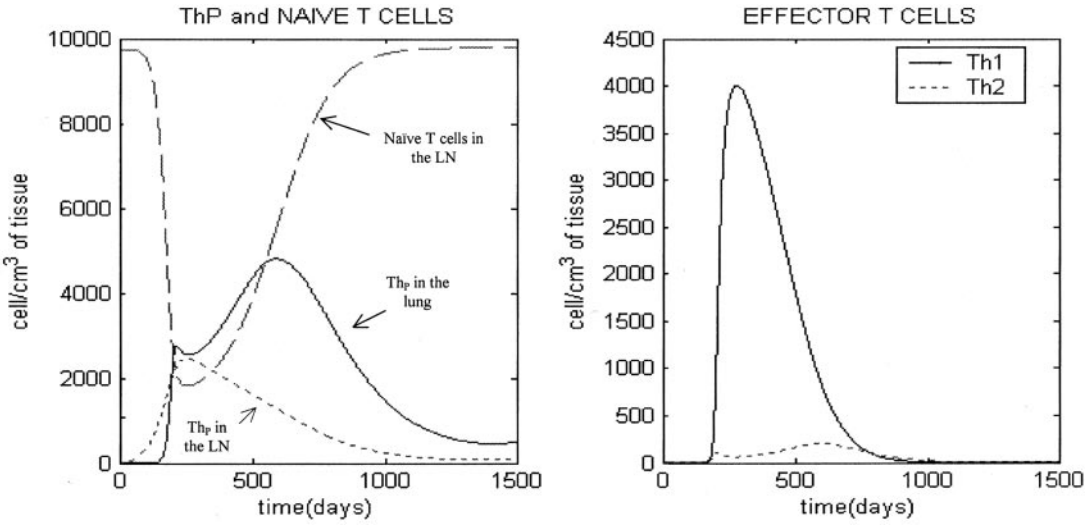

FIGURE 4. Lymphocytes (naive Ts, ThP in the lung and in the DLN, and Th1/Th2) during latency (1500 days).

Table II. *NHP data: monocyte gates of six NHPs sacrificed at different stage of disease and at different days postinfection (PI)* [a]

Stage of Disease at Necropsy	Time of Necropsy (days PI)	Lung (% $CD11b^+$)	
		Lung lobes	BAL
Minimal (1)	446	≅13	20
Minimal/moderate (3)	64–446	≅40	15–72
Advanced (2)	233–288	10–30	10–30

[a] In the first column, in parentheses, is shown the number of NHPs sacrificed. Second column shows different days PI. In the third column are shown percentages of $CD11b^+$ (monocyte gates) in BAL samples and lung tissue.

a very high percentage). To compare NHP data with our model simulations, we scaled our virtual experiment data according to the percentages given above, namely, model simulations represent 20–40% and 10–20% of the cell populations in the lung and lymph node, respectively. Table III shows our virtual experiments of Mϕ, DC, and lymphocyte population percentages in the lung and LN during latency and active TB at different days postinfection.

Our model simulations give Mϕ population percentages very similar to NHP data (both for latency and active TB). In fact, the Mϕ percentage predicted by our model during latency is between 18 and 38% (considering an interval of ~400 days, from 70 to 450 days postinfection; see Table III) compared with an interval of 13–40% of the NHP data (see Table II, Lung lobes). We obtain similar values for active TB simulations (namely, between 14 and 38.4% within the same time frame; see Table III). These results are very similar to the 10–30% interval suggested by the NHP data (Table II, Lung lobes). Our model also has the advantage to discriminate between different Mϕ subpopulations (resting, infected, and activated), giving additional information that could be tested in future experimental studies. Table IV shows data of percentages of p55 Ag-positive cells (immunohistochemically stained) over total cells calculated from images of 10 granulomas in the infected lung of two NHPs. Each value in the table represents an average of five percentages calculated on five images per granuloma.

Tables V and VI show a comparison between our mathematical model simulations and NHP data. Lymphocyte numbers are obtained from the lymphocyte gate ($CD4^+CD3^+$) of Mtb-infected lung of two representative NHPs with minimal/moderate TB disease at necropsy. DC numbers in the lung are taken from Table IV. DC numbers in the lymph node are obtained from a monocyte gate ($CD11c^+$) of the infected lung of three representative NHPs with minimal/moderate disease at necropsy. Intervals for our model simulations are obtained from Table III.

Table IV. *NHP data: percentages of p55 Ag-positive cells (immunohistochemically stained) over total cells calculated from images of 10 granulomas in the infected lungs of two NHPs*[a]

Stage of Disease at Necropsy	Granuloma	Percentage of $p55^+$ Cells[b]	SD
Advanced TB (M15300)	No. 1	10.06	1.99
	No. 2	9.27	2.53
	No. 3	10.82	0.38
	No. 4	8.07	3.82
	No. 5	8.55	0.70
	No. 6	8.17	1.23
	No. 7	8.77	1.50
	No. 8	9.74	1.49
	No. 9	9.02	2.63
Minimal/Moderate TB (M7100)	No. 1	8.17	0.86
Average		9.06	1.71
CI 95%[c]		(5.64–12.49)	

[a] One NHP with advanced disease (M153-00) and the other with minimal/moderate disease (M71-00).
[b] Average percentage of five images per granuloma. See Ref. 67 for details.
[c] CI, Confidence interval.

Our model simulations are in line with NHP $CD4^+$ cell data in the lung during latent TB infection: they are both <1%. In contrast, our model simulations underestimate lymphocyte number in the lymph node. NHP data of $CD4^+$ cells in the lymph node samples are very high (comparing with the lung): ~36%, but with a large variation (SD, ±14.11; see Table V). Our model simulations give values between 3.2 and 19.6%. This is likely due to the fact that $CD8^+$ T cells, memory T cells, and many other T cell subpopulations are not presently represented in the lymph node compartment of our model and also that our virtual experiments only simulate the number of Mtb-specific Th cells.

Regarding DC population levels in the lung, Table VI gives a confidence interval (95%) of 5.46–12.49% for the average percentage of $p55^+$ cells in two Mtb-infected NHPs (with active TB). We use this interval to approximate the number of granuloma cells that express a DC phenotype. Our model simulations (see Table VI) gives values for DCs in the lung (IDCs) between 1 and 3.6% in latency and 0.6–10% in active TB (considering an interval of ~400 days, from days 70 to 450 postinfection). This slight underestimation is likely due to the way that measurements are performed in granulomatous tissues on NHPs. Our model includes only IDCs in the lung, and p55 could account for a MDC phenotype as well. However, these data suggest that both IDCs and MDCs may be present at the site of infection.

Table III. *Latent and active TB: mathematical model simulations of macrophage, DC, and lymphocyte percentages (over the total number of cells) per 1 cm^3 of tissue (in the lung and lymph node) at different days postinfection*

Days	Mϕ (%)				DCs (%)		Lymphocytes (%)	
	Total	Resting	Activated	Infected	Lung	Lymph node	Lung	Lymph node
Latent TB								
70	18–36	18–36			1.8–3.6	0.1–0.2	0.2–0.4	9.9–19.6
200	18.2–36.4	17.4–34.8	0.6–1.4	0.2–0.4	1.6–3.2	5–10	0.2–0.4	5–6.5
300	18.4–36.8	16.2–32.4	2.2–4.4	0.2–0.4	1.2–2.4	6.8–13.6	0.4–0.8	3.2–4.2
450	19–38	16.6–33.2	2.2–4.4	0.2–0.4	1–2	4–8	0.2–0.4	6–7.6
Active TB								
70	18.6–37.2	14.4–28.8	3.6–7.2	4.6–9.2	1–2	7.6–15.2	0.4–0.8	2.4–4.8
200	19.2–38.4	11.2–22.4	6.4–12.8	1.6–3.2	0.6–1.2	8–16	0.2–0.4	2–4
300	16–32	2.8–5.6	3.2–6.4	10–20	3–6	8.3–16.6	1–2	1.7–3.4
450	14–28	3.2–6.4	3–6	8–16	5–10	8.4–16.8	1–2	1.6–3.2

Table V. *Comparisons between our mathematical model simulations and NHP lymphocyte data* [a]

	NHP Data		Mathematical Model			
	Minimal/moderate TB		Latent TB		Active TB	
	Lung	Lymph node	Lung	Lymph node	Lung	Lymph node
Lymphocyte ($CD4^+$)	0.42 ± 0.48	35.95 ± 14.11	0.2–0.8	3.2–19.6	0.2–2	1.6–4.8

[a] NHP data are expressed as average percentage ± SD. Lymphocyte numbers are obtained from a lymphocyte gate (percentages of $CD4^+CD3^+$ over 10^6 cells) of *M. tuberculosis*-infected lungs of two representative NHPs with minimal/moderate TB disease at necropsy.

DC percentages in the lymph node (MDCs) of our virtual experiments are between 0.1 and 13.6% in latency, and 7.6 and 16.8% in active TB. Tables V and VI give a confidence interval (95%) of 0.195–3.355% for the average percentage of $CD11c^+$ cells in the lymph node (minimal/moderate TB). CD11c Ab stains basically MDC phenotype (88).

Considering the bacterial load, Table VII compares CFU data collected in 17 Mtb-infected NHPs (67) with our model simulations. Represented are three different infection progressions, namely, rapid TB (10 wk), active TB (from 4 mo up to 1 year), and latency (no sign of disease in the first 6 mo). Because data are expressed per gram of tissue, we assume that 1 cm^3 approximates 1 g of tissue (both in the lung and in the hilar lymph node). One subject experienced rapid TB, eight experienced active/chronic TB, and eight experienced latent TB. Two latently infected primates had reactivation, whereas one of the eight active/chronic TB cases resolved infection only after 1 year (see Table I in Ref. 67 for details about monkey labels and stage of disease at necropsy for each monkey).

We also assume that, during disease, CFUs in the lung are mostly represented by extracellular bacteria, because numbers are much larger than intracellular. CFUs in granuloma alone likely represent a good estimate of intracellular bacteria. To determine number of bacteria in the hilar lymph node, we hypothesize that each MDC has internalized up to 10 bacteria. Our model gives results that are in line with our NHP experiments. Latency is particularly interesting: it reflects the absence of extracellular bacteria in the lung and supports the idea that "good" granuloma formation could contain infection (all bacteria are intracellular or below the level of detection).

Virtual deletion experiments

We use our model to explore mechanisms behind both cell and cytokine dynamics. We study cytokines IFN-γ, IL-12, and IL-10, and we explore DC and $CD4^+$ T cells, all through virtual deletion experiments. IL-12 deletion is performed both at the site of infection and in the DLN. The advantage of our model is that we were able to perform virtual knockout experiments that are presently difficult or impossible to do experimentally (such as DC and Th1 deletion).

Our virtual IFN-γ deletion (data not shown; see Ref. 65) shows a lack in Mϕ activation, with no Th_P migration occurring into the lung due to the very low chemokine gradient present at the site of infection (produced by activated Mϕs). Without IFN-γ, they are unable to activate Mϕs, and an exponential growth in extracellular bacteria (100-fold higher than latency) occurs. This is confirmed in mouse and human infections (89–92) where active TB results. Similar results occur for virtual IL-12 deletion (data not shown; see Ref. 65). IL-10 depletion supports the idea of a regulatory role for IL-10 (93, 94). Without IL-10, the system undergoes an abnormal increase in resident and activated Mϕs (data not shown; see Ref. 65), likely leading to a large inflammatory response or increased risk of reactivation.

All of the figures to follow represent the immune response at the site of infection of lung (*A*) and in the DLN environment (*B*). They are both scaled to cells per cubic centimeter of tissue (except for cytokines that are measured in picograms per milliliter), but in panels *A*, we refer to BAL, and in panels *B*, to cells per gram of tissue. In general, panels *A* comprise four subplots describing Mϕ populations, cytokine concentrations, Th1 and Th2 cells, and bacterial subpopulations, respectively. Panels *B* illustrate DC dynamics, naive T cells, IL-12 in the DLN, and Th_P trafficking. Although Th_P^{LUNG} and IDC belong to the lung compartment, they have been included in panels *B* to compare trafficking and migration patterns of DCs and Th_P between the lung and the DLN.

We perform two virtual DC deletion experiments. In the first experiment, we halt recruitment of new IDCs to the site of infection and prevent IDC migration to the DLN (Fig. 5). In the other experiment (data not shown), we set the IDC population in the lung to zero from the beginning and keep it zero ("complete" DC depletion). Both types of DC deletion experiments lead to an absence of T cell-mediated immunity (no Ag presentation occurs in the DLN), with an extracellular bacterial burst in <500 days (Fig. 5*A*). The same scenario occurs when $CD4^+$ T cells are deleted using our model (data not shown), where a lack of T cell immunity is not compensated for by innate immunity (Ag uptake by IDC at the site

Table VI. *Comparisons between our mathematical model simulations and NHP DC data* [a]

	NHP Data		Mathematical Model			
	Active TB	Minimal/moderate TB	Latent TB		Active TB	
	Lung	Lymph node	IDC[b]	MDC[c]	IDC[b]	MDC[c]
DCs	9.06 ± 1.71	1.775 ± 0.79	1–3.6	0.1–13.6	0.6–10	7.6–16.8

[a] DC numbers in the lung are from Table IV. DC numbers in the lymph node are percentages of $CD11c^+$ over total cells ($\cong 10^6$) in monocyte gates of the infected lung of three representative NHPs (monkey M111-01, M224-02, and M245-02) with minimal/moderate disease at necropsy. Intervals for our model simulations are obtained from Table III.

[b] IDCs are in the lung.

[c] MDCs are in the lymph node.

Table VII. *CFUs per gram of tissue (~1 cm^3)*

Location	Rapid TB (1)[a]		Active TB (8)[a]		Latency (8)[a]	
	NHP (≅70 days)	Math model (≅70 days)	NHP (120–450 days)	Math model (≅240 days)	NHP (no disease up to 200 days)	Math model (≅300 days)
Lung (extracellular)	$\cong 3 \times 10^5$	$\cong 10^6$	$\cong 2 \times 10^4$	$\cong 1.5 \times 10^4$	<LOD[b]	≅230
Granuloma (intracellular)	$\cong 10^5$	$\cong 5 \times 10^5$	$\cong 3 \times 10^5$	$\cong 8 \times 10^5$	$\cong 10^3$	$\cong 3.7 \times 10^3$
LN (total): 1–10 Mtb per mature DC	$\cong 10^5$	$\cong 10^4$–10^5	$\cong 5 \times 10^3$	$\cong 10^4$–10^5	$\cong 10^3$	$\cong 10^2$–10^3

[a] In parentheses is the number of NHPs.
[b] LOD, Level of detection.

of infection), and leads to an exponential increase of extracellular bacteria (data not shown; same as Fig. 5*A*). We also explore virtual deletions of specific subsets of lymphocytes, namely, Th1 cells (data not shown). These results highlight how a protective Th1 immunity is necessary in establishing latency, and that a Th2 response is not protective (data not shown).

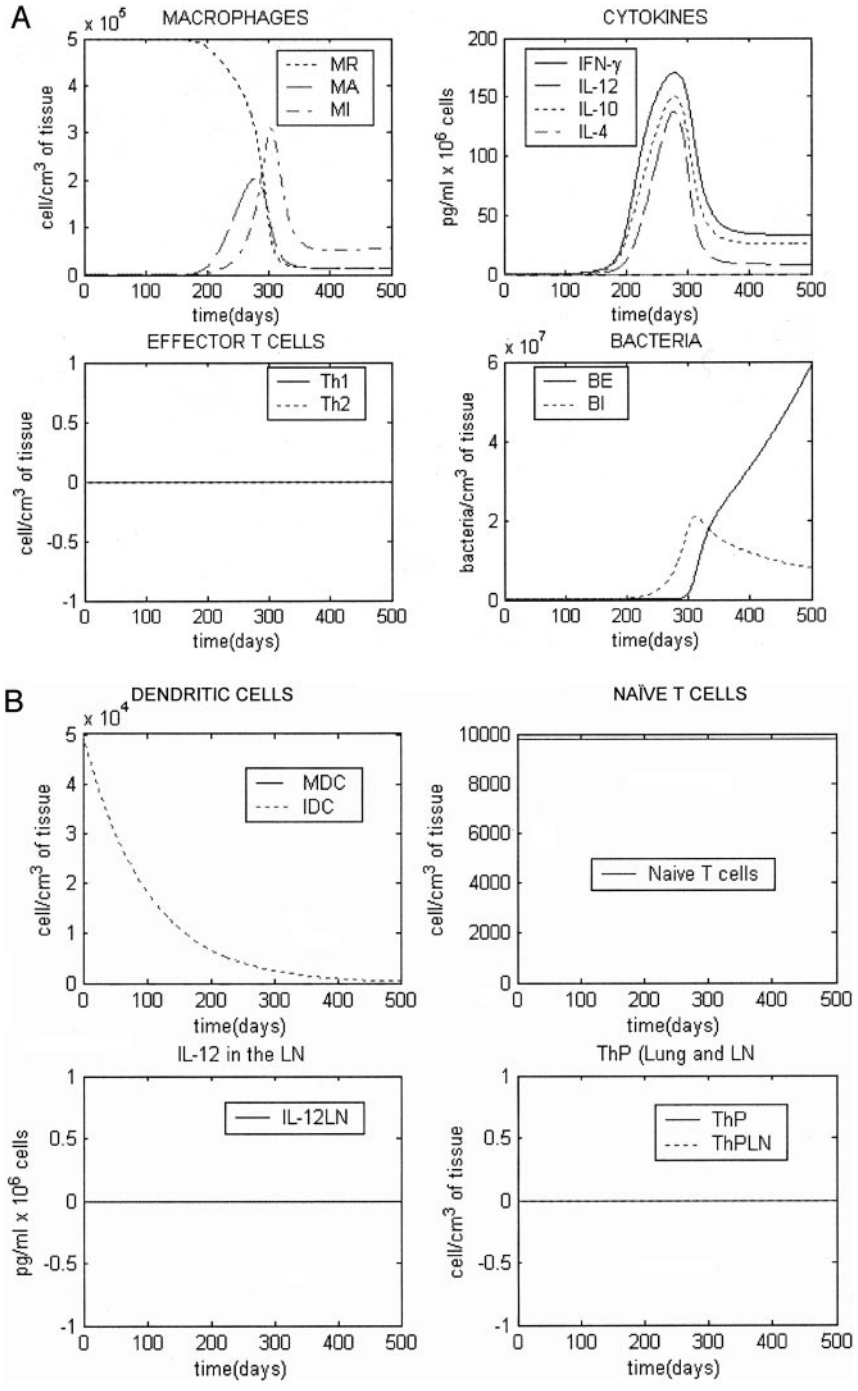

FIGURE 5. DC deletion. *A*, Lung compartment. *B*, DLN compartment. DC deletion is performed by halting recruitment of new IDCs to the site of infection and preventing IDC migration to the DLN.

Virtual depletion experiments

We use our model also to make predictions by performing a virtual depletion of different cytokines and cells (IFN-γ, IL-12, and IL-10), DC, $CD4^+$ T cells (MHC II), and Th1 cells, respectively. Depletions are performed after 1000 days (after the system achieves latency): infection outcome after depletion indicates what likely contributes to maintaining latency or inducing reactive disease.

In the latent model of infection, $CD4^+$ T cells, NO synthase, and TNF-α have been demonstrated to be necessary to maintain control of infection (3). Depletion of IFN-γ and IL-12 throws the system out of latency into active disease reactivation.

In fact, depletion of IFN-γ and IL-12 causes a drastic decrease in both activated Mϕ and T cell populations, with extracellular bacteria increasing to uncontrollable levels that cannot be compensated for by DC trafficking and presentation (data not shown). This is in line with several $CD4^+$ deletion/depletion experimental data (3, 95–97) and confirms our virtual deletion simulation results.

We are able to perform two different virtual DC depletion that cannot be done experimentally. The first experiment is performed by setting to zero both IDC recruitment at the site of infection and IDC migration to the DLN (at 1000 days postinfection), thus eliminating any possibility of additional Ag presentation and T cell immunity (partial DC depletion). The other experiment sets the IDC population

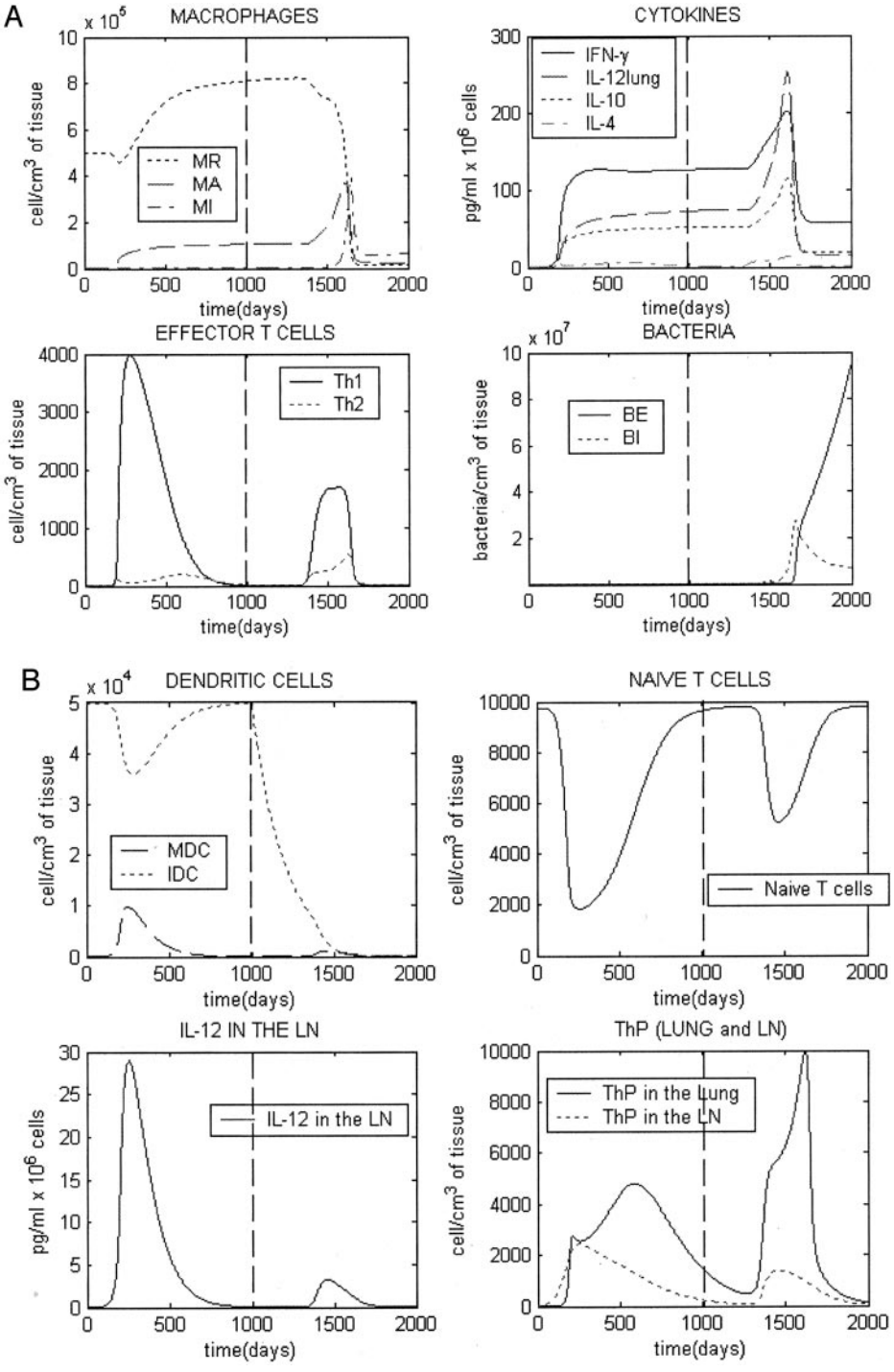

FIGURE 6. DC depletion. *A*, Lung compartment. *B*, DLN compartment. The system is in latency (see Figs. 2–4) until depletion is performed (represented by the vertical line at day 1000). This partial DC depletion is performed by eliminating IDC recruitment at the site of infection and IDC migration to the DLN.

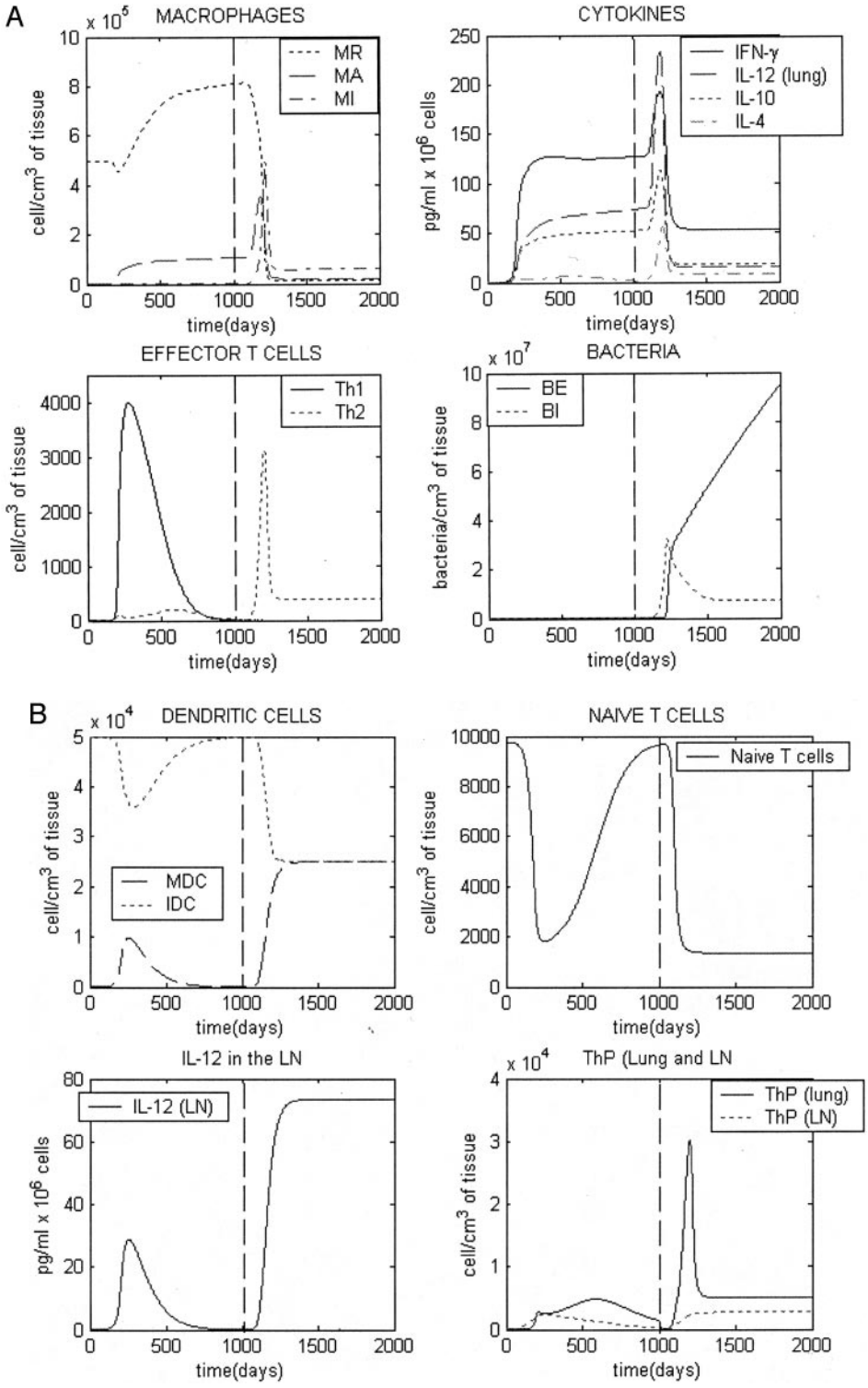

FIGURE 7. Th1 depletion. *A*, Lung compartment. *B*, DLN compartment. The system is in latency (see Figs. 2–4) until depletion is performed (represented by the vertical line at day 1000). This depletion is performed by eliminating Ag presentation in the DLN by MDC.

in the lung to zero ("complete" DC depletion), after 1000 days. Both DC depletion experiments lead to reactivation, but in the case of partial DC depletion experiment (Fig. 6), there is an interesting trade-off between IDCs and extracellular bacteria: the longer it takes to deplete the IDC population at the site of infection (which depends on the IDC death rate, because we halted IDC recruitment), the higher the possibility of enhancing a second wave of effector T cell response at the site of infection (Fig. 6*A*, Effector Cell plots). Because the resident IDC population will eventually deplete, progression to primary TB is just a matter of time. This also could induce reactivation or chronic infection scenarios.

Because in our model we do not include memory T cells, the level of T cell immunity is determined by the level of priming of new T cells and T cell proliferation. Thus, $CD4^+$ T cell (MHC II) depletion is performed by depleting MDC presentation in the DLN (after 1000 days), and it leads to primary TB (data not shown, outcome similar to Th1 virtual depletion experiment of Fig. 7). Again, using our virtual infection model, we are able to deplete a specific subset of lymphocytes, namely Th1 cells (it cannot currently be done experimentally). This result is in line with the CD4 and Th1 virtual deletion experiment (data not shown) and highlights how a protective Th1 immunity is necessary in maintaining latency,

Table VIII. *Parameter classification and sensitivity analysis (DCs and trafficking)*[a]

Parameters	Action	Event
Presentation/activation/differentiation		
IL-12 production by MDC, in the DLN	Decrease (2- to 20-fold)	From latency to disease
MDC death and exhaustion rate	Increase (1- to 100-fold)	From latency to disease
MDC-T cell interactions: T cell activation	Decrease (10- to 100-fold)	From latency to disease
Trafficking		
% of precursor Th cells migrating out of the DLN into the blood	Decrease (from 90 to 10%)	From latency to primary TB
IDC normal turnover in the lung	Decrease (1- to 100-fold)	From latency to disease
IDC activation/migration/maturation from the lung to the DLN	Decrease (1- to 50-fold)	From latency to disease (high levels of B_I and B_E, 10^7)
IDC activation/migration/maturation from the lung to the DLN	Increase (1- to 100-fold)	From latency to B_I, 10-fold lower
Uptake/killing		
IDC uptake of B_E	Increase (10- to 200-fold)	From latency to clearance

[a] B_E, Extracellular bacteria; B_I, intracellular bacteria.

even though it may be very low, and the absence of this response leads to reactivation (Fig. 7*A*).

Mechanisms leading to different infection outcomes

To determine which mechanisms in the model control whether the system progresses to latency or to active disease, we performed a detailed uncertainty and sensitivity analysis on all parameters in the system (see *Materials and Methods*). Surprisingly, of the 50 interactions in the model, only a handful are determinative in infection outcome. In a previous study (65), we showed the importance of infectivity and uptake/killing parameters in establishing and maintaining latency. To better understand the role of DCs in Mtb infection, we classify the mechanisms (based on the parameters that determine the terms) into three groups, namely, presentation/activation/differentiation, trafficking, and uptake/killing parameters (see Table VIII). The importance of DCs in determining latency is supported by a key role for factors involved in Ag presentation. In fact, primary TB results if the level of MDC-T cell interaction in the T cell area of the DLN is decreased or if the MDC death rate is increased (that could be due to a faster MDC death rate or faster rate of "exhaustion" of MDCs in the DLN).

A key role for MDC activity in the DLN is also supported by the importance of the parameter regulating the production of IL-12 by MDCs. If this rate is decreased, primary TB occurs, and this is due to a lack of Th1 response. New data in a mouse model lacking CD40 support this finding (98). However, if we decrease the two main DC trafficking parameters, namely, the maximal rate of migration of IDC to the DLN and the percentage of precursor Th cells migrating out of the DLN into the blood, fast progressive infection occurs. This is again a result of reduced adaptive immunity at the site of infection.

This suggests that a delay in DC and T cell trafficking can alter the outcome of Mtb infection. Moreover, the protective innate role of DCs as a reservoir for Mtb bacteria during latency is confirmed by the relevance of the parameter governing the normal turnover rate of IDCs at the site of infection: decreasing this rate results in a constant but continuous increase in bacterial load ("slow" infection or a possible reactivation scenario).

Discussion

In this study, we coupled a NHP model with a virtual infection model of the human immune response to Mtb (65) to examine the role of DC trafficking between the site of infection (lung) and the secondary lymphoid tissue (lymph node) in determining the infection outcome.

Our model simulations highlight the role of phagocytic cells (Mϕs and DCs) in initiating and directing adaptive T cell immunity, in particular, the key action of DCs in establishing and maintaining latency. DCs have multiple roles: they participate in innate immunity by internalizing bacteria at the site of infection and represent the main link between innate and adaptive immunity via trafficking from lung to lymph node.

The first stage of infection begins with inhalation of tubercle bacilli. Resident Mϕs and IDCs in the lung ingest bacilli and likely often clear them (via innate immunity). There are multiple mechanisms for the uptake of Mtb, involving a number of different host cell receptors (99), and distinct routes of entry may lead to differences in signal transduction, immune activation, and intracellular survival. For example, the main Mtb receptors on Mϕs are complement receptor 3 and mannose receptor, whereas recent evidence suggests that DC-SIGN is a primary Mtb receptor on DCs (100). Virulent strains of Mtb are phagocytosed through the mannose receptor, whereas attenuated strains are not (101), suggesting that a different route of entry might be advantageous to mycobacteria, and that DC-SIGN-mediated entry into DCs likely influences bacterial persistence and host immunity (100). In vivo, the possible role of these events in immune evasion by Mtb remains to be determined. Our model suggests how increasing the rate of bacterial uptake by resident IDCs could be advantageous both in terms of a stronger innate response and as a more efficient link to an effective adaptive response.

To validate our model simulations, Mtb-infected NHP have been studied. Mϕ and DC percentages resulting from our model simulations are very similar to the NHP experimental data. Moreover, CFU data are in line with our simulations, especially in latently infected NHPs, where the absence of Mtb in the lung of latently infected primates suggests that the total bacterial load is intracellular and contained within granulomas.

Our simulations indicate that DCs are necessary in establishing protective immunity and in containing infection. The main result of this work is that a delay either in DC migration to the DLN or T cell trafficking to the site of infection can alter the outcome of Mtb infection (see Table VII) or define a progression from latency to active TB or a possible reactivation scenario. Delayed DC migration can be simulated in our model by decreasing IDC turnover rates or IDC migration rates from the site of infection to the DLN. T cell trafficking can be altered by decreasing the percentage of precursor Th cells migrating out of the DLN. We can also modulate the intensity and duration of Ag presentation in the DLN by changing MDC-naive T cell interaction term or MDC half-life,

respectively. Our results are in line with the idea that a fast DC turnover at the site of infection, as well as strong activation of DCs leading to maximal Ag presentation and production of key cytokines (inducing the most protective T cell response), could represent a viable strategy for the development of a new generation of treatments against Mtb (35, 102–107).

References

1. Arend, S. M., and J. T. van Dissel. 2002. Evidence of endogenous reactivation of tuberculosis after a long period of latency. *J. Infect. Dis. 186:876*.
2. Lillebaek, T., A. Dirksen, I. Baess, B. Strunge, V. O. Thomsen, and A. B. Andersen. 2002. Molecular evidence of endogenous reactivation of *Mycobacterium tuberculosis* after 33 years of latent infection. *J. Infect. Dis. 185:401*.
3. Flynn, J. L., and J. Chan. 2001. Tuberculosis: latency and reactivation. *Infect. Immun. 69:4195*.
4. Tufariello, J. M., J. Chan, and J. L. Flynn. 2003. Latent tuberculosis: mechanisms of host and bacillus that contribute to persistent infection. *Lancet Infect. Dis. 3:578*.
5. Styblo, K. 1980. Recent advances in epidemiological research in tuberculosis. *Adv. Tuberc. Res. 20:1*.
6. Comstock, G. W., V. T. Livesay, and S. F. Woolpert. 1974. The prognosis of a positive tuberculin reaction in childhood and adolescence. *Am. J. Epidemiol. 99:131*.
7. Bloom, B. R. 1994. *Tuberculosis: Pathogenesis, Protection, and Control.* Am. Soc. Microbiol., Washington, DC.
8. Bottomly, K. 1999. T cells and dendritic cells get intimate. *Science 283:1124*.
9. Lanzavecchia, A., and F. Sallusto. 2000. Dynamics of T lymphocyte responses: intermediates, effectors, and memory cells. *Science 290:92*.
10. Mellman, I., and R. M. Steinman. 2001. Dendritic cells: specialized and regulated antigen processing machines. *Cell 106:255*.
11. De Smedt, T., E. Butz, J. Smith, R. Maldonado-Lopez, B. Pajak, M. Moser, and C. Maliszewski. 2001. CD8α^- and CD8α^+ subclasses of dendritic cells undergo phenotypic and functional maturation in vitro and in vivo. *J. Leukocyte Biol. 69:951*.
12. Grabbe, S., E. Kampgen, and G. Schuler. 2000. Dendritic cells: multi-lineal and multi-functional. *Immunol. Today 21:431*.
13. Liu, Y. J., N. Kadowaki, M. C. Rissoan, and V. Soumelis. 2000. T cell activation and polarization by DC1 and DC2. *Curr. Top. Microbiol. Immunol. 251:149*.
14. Maldonado-Lopez, R., T. De Smedt, B. Pajak, C. Heirman, K. Thielemans, O. Leo, J. Urbain, C. R. Maliszewski, and M. Moser. 1999. Role of CD8α^+ and CD8α^- dendritic cells in the induction of primary immune responses in vivo. *J. Leukocyte Biol. 66:242*.
15. Maldonado-Lopez, R., T. De Smedt, P. Michel, J. Godfroid, B. Pajak, C. Heirman, K. Thielemans, O. Leo, J. Urbain, and M. Moser. 1999. CD8α^+ and CD8α^- subclasses of dendritic cells direct the development of distinct T helper cells in vivo. *J. Exp. Med. 189:587*.
16. Maldonado-Lopez, R., and M. Moser. 2001. Dendritic cell subsets and the regulation of Th1/Th2 responses. *Semin. Immunol. 13:275*.
17. Maldonado-Lopez, R., C. Maliszewski, J. Urbain, and M. Moser. 2001. Cytokines regulate the capacity of CD8α^+ and CD8α^- dendritic cells to prime Th1/Th2 cells in vivo. *J. Immunol. 167:4345*.
18. Moser, M., and K. M. Murphy. 2000. Dendritic cell regulation of TH1-TH2 development. *Nat. Immunol. 1:199*.
19. Pulendran, B., J. L. Smith, G. Caspary, K. Brasel, D. Pettit, E. Maraskovsky, and C. R. Maliszewski. 1999. Distinct dendritic cell subsets differentially regulate the class of immune response in vivo. *Proc. Natl. Acad. Sci. USA 96:1036*.
20. Rissoan, M. C., V. Soumelis, N. Kadowaki, G. Grouard, F. Briere, R. de Waal Malefyt, and Y. J. Liu. 1999. Reciprocal control of T helper cell and dendritic cell differentiation. *Science 283:1183*.
21. Schlecht, G., C. Leclerc, and G. Dadaglio. 2001. Induction of CTL and nonpolarized Th cell responses by CD8α^+ and CD8α^- dendritic cells. *J. Immunol. 167:4215*.
22. Medzhitov, R., and C. A. Janeway, Jr. 1997. Innate immunity: the virtues of a nonclonal system of recognition. *Cell 91:295*.
23. Arriaga, A. K., E. H. Orozco, L. D. Aguilar, G. A. Rook, and R. Hernandez Pando. 2002. Immunological and pathological comparative analysis between experimental latent tuberculous infection and progressive pulmonary tuberculosis. *Clin. Exp. Immunol. 128:229*.
24. Matzinger, P. 2002. An innate sense of danger. *Ann. NY Acad. Sci. 961:341*.
25. Matzinger, P. 2002. The danger model: a renewed sense of self. *Science 296:301*.
26. Rescigno, M., and P. Borrow. 2001. The host-pathogen interaction: new themes from dendritic cell biology. *Cell 106:267*.
27. Rescigno, M. 2002. Dendritic cells and the complexity of microbial infection. *Trends Microbiol. 10:425*.
28. Rescigno, M., M. Urbano, M. Rimoldi, B. Valzasina, G. Rotta, F. Granucci, and P. Ricciardi-Castagnoli. 2002. Toll-like receptor 4 is not required for the full maturation of dendritic cells or for the degradation of Gram-negative bacteria. *Eur. J. Immunol. 32:2800*.
29. Fernandez, N. C., C. Flament, F. Crepineau, E. Angevin, E. Vivier, and L. Zitvogel. 2002. Dendritic cells (DC) promote natural killer (NK) cell functions: dynamics of the human DC/NK cell cross talk. *Eur. Cytokine Netw. 13:17*.
30. Gallucci, S., M. Lolkema, and P. Matzinger. 1999. Natural adjuvants: endogenous activators of dendritic cells. *Nat. Med. 5:1249*.
31. Reis e Sousa, C. 2001. Dendritic cells as sensors of infection. *Immunity 14:495*.
32. Pulendran, B., K. Palucka, and J. Banchereau. 2001. Sensing pathogens and tuning immune responses. *Science 293:253*.
33. Kalinski, P., C. M. Hilkens, E. A. Wierenga, and M. L. Kapsenberg. 1999. T-cell priming by type-1 and type-2 polarized dendritic cells: the concept of a third signal. *Immunol. Today 20:561*.
34. Flynn, J. L., and J. Chan. 2001. Immunology of tuberculosis. *Annu. Rev. Immunol. 19:93*.
35. Giacomini, E., E. Iona, L. Ferroni, M. Miettinen, L. Fattorini, G. Orefici, I. Julkunen, and E. M. Coccia. 2001. Infection of human macrophages and dendritic cells with *Mycobacterium tuberculosis* induces a differential cytokine gene expression that modulates T cell response. *J. Immunol. 166:7033*.
36. Feng, C. G., C. Demangel, A. T. Kamath, M. Macdonald, and W. J. Britton. 2001. Dendritic cells infected with *Mycobacterium bovis* bacillus Calmette-Guérin activate CD8$^+$ T cells with specificity for a novel mycobacterial epitope. *Int. Immunol. 13:451*.
37. Bodnar, K. A., N. V. Serbina, and J. L. Flynn. 2001. Fate of *Mycobacterium tuberculosis* within murine dendritic cells. *Infect. Immun. 69:800*.
38. Demangel, C., and W. J. Britton. 2000. Interaction of dendritic cells with mycobacteria: where the action starts. *Immunol. Cell Biol. 78:318*.
39. Hickman, S. P., J. Chan, and P. Salgame. 2002. *Mycobacterium tuberculosis* induces differential cytokine production from dendritic cells and macrophages with divergent effects on naive T cell polarization. *J. Immunol. 168:4636*.
40. Jiao, X., R. Lo-Man, P. Guermonprez, L. Fiette, E. Deriaud, S. Burgaud, B. Gicquel, N. Winter, and C. Leclerc. 2002. Dendritic cells are host cells for mycobacteria in vivo that trigger innate and acquired immunity. *J. Immunol. 168:1294*.
41. Holt, P. G., and M. A. Schon-Hegrad. 1987. Localization of T cells, macrophages and dendritic cells in rat respiratory tract tissue: implications for immune function studies. *Immunology 62:349*.
42. Holt, P. G., J. Oliver, N. Bilyk, C. McMenamin, P. G. McMenamin, G. Kraal, and T. Thepen. 1993. Downregulation of the antigen presenting cell function(s) of pulmonary dendritic cells in vivo by resident alveolar macrophages. *J. Exp. Med. 177:397*.
43. Holt, P. G. 2000. Antigen presentation in the lung. *Am. J. Respir. Crit. Care Med. 162:S151*.
44. Sertl, K., T. Takemura, E. Tschachler, V. J. Ferrans, M. A. Kaliner, and E. M. Shevach. 1986. Dendritic cells with antigen-presenting capability reside in airway epithelium, lung parenchyma, and visceral pleura. *J. Exp. Med. 163:436*.
45. van Haarst, J. M., H. J. de Wit, H. A. Drexhage, and H. C. Hoogsteden. 1994. Distribution and immunophenotype of mononuclear phagocytes and dendritic cells in the human lung. *Am. J. Respir. Cell Mol. Biol. 10:487*.
46. Guermonprez, P., J. Valladeau, L. Zitvogel, C. Thery, and S. Amigorena. 2002. Antigen presentation and T cell stimulation by dendritic cells. *Annu. Rev. Immunol. 20:621*.
47. Banchereau, J., and R. M. Steinman. 1998. Dendritic cells and the control of immunity. *Nature 392:245*.
48. Banchereau, J., F. Briere, C. Caux, J. Davoust, S. Lebecque, Y. J. Liu, B. Pulendran, and K. Palucka. 2000. Immunobiology of dendritic cells. *Annu. Rev. Immunol. 18:767*.
49. Gonzalez-Juarrero, M., and I. M. Orme. 2001. Characterization of murine lung dendritic cells infected with *Mycobacterium tuberculosis*. *Infect. Immun. 69:1127*.
50. Havenith, C. E., A. J. Breedijk, and E. C. Hoefsmit. 1992. Effect of bacillus Calmette-Guérin inoculation on numbers of dendritic cells in bronchoalveolar lavages of rats. *Immunobiology 184:336*.
51. Henderson, R. A., S. C. Watkins, and J. L. Flynn. 1997. Activation of human dendritic cells following infection with *Mycobacterium tuberculosis*. *J. Immunol. 159:635*.
52. Palucka, K., and J. Banchereau. 1999. Linking innate and adaptive immunity. *Nat. Med. 5:868*.
53. Choi, Y. K., B. A. Fallert, M. A. Murphey-Corb, and T. A. Reinhart. 2002. Simian immunodeficiency virus dramatically alters expression of homeostatic chemokines and dendritic cell markers during infection in vivo. *Blood 24:24*.
54. Sallusto, F., P. Schaerli, P. Loetscher, C. Schaniel, D. Lenig, C. R. Mackay, S. Qin, and A. Lanzavecchia. 1998. Rapid and coordinated switch in chemokine receptor expression during dendritic cell maturation. *Eur. J. Immunol. 28:2760*.
55. Lanzavecchia, A., and F. Sallusto. 2001. Regulation of T cell immunity by dendritic cells. *Cell 106:263*.
56. Lanzavecchia, A. 1999. Dendritic cell maturation and generation of immune responses. *Haematologica 84(Suppl. EHA-4):23*.
57. Janeway, C. 2001. *Immunobiology 5: The Immune System in Health and Disease*. Garland, New York.
58. Zhu, K., Q. Shen, M. Ulrich, and M. Zheng. 2000. Human monocyte-derived dendritic cells expressing both chemotactic cytokines IL-8, MCP-1, RANTES and their receptors, and their selective migration to these chemokines. *Chin. Med. J. (Engl.) 113:1124*.
59. Adema, G. J., F. Hartgers, R. Verstraten, E. de Vries, G. Marland, S. Menon, J. Foster, Y. Xu, P. Nooyen, T. McClanahan, et al. 1997. A dendritic-cell-derived C-C chemokine that preferentially attracts naive T cells. *Nature 387:713*.
60. DesJardin, L. E., T. M. Kaufman, B. Potts, B. Kutzbach, H. Yi, and L. S. Schlesinger. 2002. *Mycobacterium tuberculosis*-infected human macrophages exhibit enhanced cellular adhesion with increased expression of LFA-1 and ICAM-1 and reduced expression and/or function of complement receptors, FcγRII and the mannose receptor. *Microbiology 148:3161*.

61. Russo, D. M., N. Kozlova, D. L. Lakey, and D. Kernodle. 2000. Naive human T cells develop into Th1 effectors after stimulation with *Mycobacterium tuberculosis*-infected macrophages or recombinant Ag85 proteins. *Infect. Immun. 68:6826*.
62. Langenkamp, A., M. Messi, A. Lanzavecchia, and F. Sallusto. 2000. Kinetics of dendritic cell activation: impact on priming of TH1, TH2 and nonpolarized T cells. *Nat. Immunol. 1:311*.
63. Fortsch, D., M. Rollinghoff, and S. Stenger. 2000. IL-10 converts human dendritic cells into macrophage-like cells with increased antibacterial activity against virulent *Mycobacterium tuberculosis*. *J. Immunol. 165:978*.
64. Palucka, K. A., N. Taquet, F. Sanchez-Chapuis, and J. C. Gluckman. 1998. Dendritic cells as the terminal stage of monocyte differentiation. *J. Immunol. 160:4587*.
65. Marino, S., and D. E. Kirschner. 2004. The human immune response to *Mycobacterium tuberculosis* in lung and lymph node. *J. Theor. Biol. 227:463.*
66. Flynn, J. L., S. V. Capuano, D. Croix, S. Pawar, A. Myers, A. Zinovik, and E. Klein. 2003. Non-human primates: a model for tuberculosis research. *Tuberculosis (Edinb.) 83:116*.
67. Capuano, S. V. III, D. A. Croix, S. Pawar, A. Zinovik, A. Myers, P. L. Lin, S. Bissel, C. Fuhrman, E. Klein, and J. L. Flynn. 2003. Experimental *Mycobacterium tuberculosis* infection of cynomolgus macaques closely resembles the various manifestations of human *M. tuberculosis* infection. *Infect. Immun. 71:5831*.
68. Gammack, D., C. R. Doering, and D. E. Kirschner. 2004. Macrophage response to *Mycobacterium tuberculosis* infection. *J. Math. Biol. 48:218.*
69. Croix, D. A., S. Capuano III, L. Simpson, B. A. Fallert, C. L. Fuller, E. C. Klein, T. A. Reinhart, M. Murphey-Corb, and J. L. Flynn. 2000. Effect of mycobacterial infection on virus loads and disease progression in simian immunodeficiency virus-infected rhesus monkeys. *AIDS Res. Hum. Retroviruses 16:1895*.
70. Sallusto, F., D. Lenig, R. Forster, M. Lipp, and A. Lanzavecchia. 1999. Two subsets of memory T lymphocytes with distinct homing potentials and effector functions. *Nature 401:708*.
71. Sallusto, F., C. R. Mackay, and A. Lanzavecchia. 2000. The role of chemokine receptors in primary, effector, and memory immune responses. *Annu. Rev. Immunol. 18:593*.
72. Sallusto, F., and A. Lanzavecchia. 2000. Understanding dendritic cell and T-lymphocyte traffic through the analysis of chemokine receptor expression. *Immunol. Rev. 177:134*.
73. Lazarevic, V., and J. Flynn. 2002. $CD8^+$ T cells in tuberculosis. *Am. J. Respir. Crit. Care Med. 166:1116*.
74. Serbina, N. V., C. C. Liu, C. A. Scanga, and J. L. Flynn. 2000. $CD8^+$ CTL from lungs of *Mycobacterium tuberculosis*-infected mice express perforin in vivo and lyse infected macrophages. *J. Immunol. 165:353*.
75. Serbina, N. V., and J. L. Flynn. 2001. $CD8^+$ T cells participate in the memory immune response to *Mycobacterium tuberculosis*. *Infect. Immun. 69:4320*.
76. Blower, S. M., and H. Dowlatabadi. 1994. Sensitivity and uncertainty analysis of complex-models of disease transmission: an HIV model, as an example. *Int. Stat. Rev. 62:229.*
77. Greenland, S. 2001. Sensitivity analysis, Monte Carlo risk analysis, and Bayesian uncertainty assessment. *Risk Anal. 21:579.*
78. Helton, J. C., and F. J. Davis. 2002. Illustration of sampling-based methods for uncertainty and sensitivity analysis. *Risk Anal. 22:591*.
79. Sanchez, M. A., and S. M. Blower. 1997. Uncertainty and sensitivity analysis of the basic reproductive rate: tuberculosis as an example. *Am. J. Epidemiol. 145:1127*.
80. Harbeck, R. J. 1998. Immunophenotyping of bronchoalveolar lavage lymphocytes. *Clin. Diagn. Lab. Immunol. 5:271*.
81. Goldstein, R. A., P. K. Rohatgi, E. H. Bergofsky, E. R. Block, R. P. Daniele, D. R. Dantzker, G. S. Davis, G. W. Hunninghake, T. E. King, Jr., W. J. Metzger, et al. 1990. Clinical role of bronchoalveolar lavage in adults with pulmonary disease. *Am. Rev. Respir. Dis. 142:481.*
82. 1989. Technical recommendations and guidelines for bronchoalveolar lavage (BAL): Report of the European Society of Pneumology Task Group. *Eur. Respir. J. 2:561.*
83. Choi, M. S., J. H. Lee, K. C. Koh, S. W. Paik, P. L. Rhee, J. J. Kim, J. C. Rhee, K. W. Choi, and S. H. Kim. 2001. Clinical significance of enlarged perihepatic lymph nodes in chronic hepatitis B. *J. Clin. Gastroenterol. 32:329.*
84. Condos, R., W. N. Rom, Y. M. Liu, and N. W. Schluger. 1998. Local immune responses correlate with presentation and outcome in tuberculosis. *Am. J. Respir. Crit. Care Med. 157:729.*
85. Taha, R. A., T. C. Kotsimbos, Y. L. Song, D. Menzies, and Q. Hamid. 1997. IFN-γ and IL-12 are increased in active compared with inactive tuberculosis. *Am. J. Respir. Crit. Care Med. 155:1135*.
86. Taha, R. A., E. M. Minshall, R. Olivenstein, D. Ihaku, B. Wallaert, A. Tsicopoulos, A. B. Tonnel, R. Damia, D. Menzies, and Q. A. Hamid. 1999. Increased expression of IL-12 receptor mRNA in active pulmonary tuberculosis and sarcoidosis. *Am. J. Respir. Crit. Care Med. 160:1119.*
87. Barnes, P. F., S. Lu, J. S. Abrams, E. Wang, M. Yamamura, and R. L. Modlin. 1993. Cytokine production at the site of disease in human tuberculosis. *Infect. Immun. 61:3482*.
88. O'Doherty, U., M. Peng, S. Gezelter, W. J. Swiggard, M. Betjes, N. Bhardwaj, and R. M. Steinman. 1994. Human blood contains two subsets of dendritic cells, one immunologically mature and the other immature. *Immunology 82:487*.
89. Cooper, A. M., D. K. Dalton, T. A. Stewart, J. P. Griffin, D. G. Russell, and I. M. Orme. 1993. Disseminated tuberculosis in interferon-γ gene-disrupted mice. *J. Exp. Med. 178:2243*.
90. Flynn, J. L., J. Chan, K. J. Triebold, D. K. Dalton, T. A. Stewart, and B. R. Bloom. 1993. An essential role for interferon-γ in resistance to *Mycobacterium tuberculosis* infection. *J. Exp. Med. 178:2249*.
91. Holland, S. M., S. E. Dorman, A. Kwon, I. F. Pitha-Rowe, D. M. Frucht, S. M. Gerstberger, G. J. Noel, P. Vesterhus, M. R. Brown, and T. A. Fleisher. 1998. Abnormal regulation of interferon-γ, interleukin-12, and tumor necrosis factor-α in human interferon-γ receptor 1 deficiency. *J. Infect. Dis. 178:1095*.
92. Newport, M. J., C. M. Huxley, S. Huston, C. M. Hawrylowicz, B. A. Oostra, R. Williamson, and M. Levin. 1996. A mutation in the interferon-γ-receptor gene and susceptibility to mycobacterial infection. *N. Engl. J. Med. 335:1941*.
93. Murray, P. J., and R. A. Young. 1999. Increased antimycobacterial immunity in interleukin-10-deficient mice. *Infect. Immun. 67:3087*.
94. Wigginton, J. E., and D. Kirschner. 2001. A model to predict cell-mediated immune regulatory mechanisms during human infection with *Mycobacterium tuberculosis*. *J. Immunol. 166:1951*.
95. Bonecini-Almeida, M. G., S. Chitale, I. Boutsikakis, J. Geng, H. Doo, S. He, and J. L. Ho. 1998. Induction of in vitro human macrophage anti-*Mycobacterium tuberculosis* activity: requirement for IFN-γ and primed lymphocytes. *J. Immunol. 160:4490*.
96. Caruso, A. M., N. Serbina, E. Klein, K. Triebold, B. R. Bloom, and J. L. Flynn. 1999. Mice deficient in CD4 T cells have only transiently diminished levels of IFN-γ, yet succumb to tuberculosis. *J. Immunol. 162:5407*.
97. Flynn, J. L., and J. D. Ernst. 2000. Immune responses in tuberculosis. *Curr. Opin. Immunol. 12:432*.
98. Lazarevic, V., A. J. Myers, C. A. Scanga, and J. L. Flynn. 2003. CD40, but not CD40L, is required for the optimal priming of T cells and control of aerosol *M. tuberculosis* infection. *Immunity 19:823*.
99. Li, Y. J., M. Petrofsky, and L. E. Bermudez. 2002. *Mycobacterium tuberculosis* uptake by recipient host macrophages is influenced by environmental conditions in the granuloma of the infectious individual and is associated with impaired production of interleukin-12 and tumor necrosis factor-α. *Infect. Immun. 70:6223*.
100. Tailleux, L., O. Schwartz, J. L. Herrmann, E. Pivert, M. Jackson, A. Amara, L. Legres, D. Dreher, L. P. Nicod, J. C. Gluckman, et al. 2003. DC-SIGN is the major *Mycobacterium tuberculosis* receptor on human dendritic cells. *J. Exp. Med. 197:121*.
101. Schlesinger, L. S. 1993. Macrophage phagocytosis of virulent but not attenuated strains of *Mycobacterium tuberculosis* is mediated by mannose receptors in addition to complement receptors. *J. Immunol. 150:2920*.
102. Iseman, M. D. 2002. Tuberculosis therapy: past, present and future. *Eur. Respir. J. Suppl. 36:87s.*
103. Iseman, M. D. 2000. *A Clinician's Guide to Tuberculosis.* Lippincott Williams & Wilkins, Philadelphia.
104. International Union against Tuberculosis and Lung Disease, World Conference, and M. D. Iseman. 1999. Update treatment of multidrug-resistant tuberculosis: proceedings of a sponsored symposium to the 29th World Conference of the International Union against Tuberculosis and Lung Diseases (IUATLD/UICTMR): Bangkok, Thailand, November 24, 1998. Karger, Basel.
105. Orme, I. M., D. N. McMurray, and J. T. Belisle. 2001. Tuberculosis vaccine development: recent progress. *Trends Microbiol. 9:115*.
106. Iseman, M. D. 2000. TB elimination in the 21st century, a quixotic dream? *Int. J. Tuberc. Lung Dis. 4:S109.*
107. Iseman, M. D. 2000. Tuberculosis: still the #1 killer in infectious diseases. *Int. J. Clin. Pract. Suppl. 78.*